# A Picosecond Kinetic Study of Nonadiabatic Proton Transfer within the Contact Radical Ion Pair of Substituted Benzophenones/*N*,*N*-Diethylaniline

**Kevin S. Peters* and Amanda Cashin**

*Department of Chemistry and Biochemistry, University of Colorado, Boulder, Colorado 80309*

*Received: November 9, 1999; In Final Form: February 28, 2000*

Picosecond absorption spectroscopy is utilized in determining the dynamics of proton transfer within a variety of substituted benzophenones/*N*,*N*-diethylaniline contact radical ion pairs in the solvents benzene and cyclohexane. A correlation of the rate constants with change in free energy for the reactions reveals an "inverted region" for proton transfer. This kinetic behavior is consistent with nonadiabatic proton transfer theories suggesting that the reaction involves proton tunneling at ambient temperatures.

## Introduction

In recent years there has been renewed interest in the development of models that describe the mechanisms by which a proton is transferred in an acid−base reaction.[1−11] The standard model, Transition State Theory, assumes a classical transition state defined by a free energy maximum along the proton-transfer reaction coordinate over which the proton passes.[12−14] However, the basic tenant of Transition State Theory has been brought into question as a result of recent theoretical studies of gas-phase proton-transfer reactions that reveal that tunneling is the dominant reaction mode for proton transfer, even at ambient temperatures.[1−3] When the effect of solvent is incorporated into the kinetic models, solution phase reactions that have an electronic barrier in the proton-transfer coordinate again are postulated to proceed by tunneling.[4−11] Given the importance of proton-transfer reactions in both chemistry and biochemistry, a reformulation of the mechanisms for proton transfer will have a profound impact on our understanding of the nature of these reaction processes.[15,16]

Although theory has been addressing the issue of tunneling as the predominate reaction mode in proton-transfer reactions for more than 20 years, there has been little significant advances, from an experimental perspective, relating to these issues for condense phase reactions.[17−29] In part, design of experiments to test the predictions of the various theoretical formulations has been exceedingly difficult. Because the rate for the tunneling of a proton is highly dependent on distance, it is necessary that the molecular systems to be studied constrain the distance of proton transfer. Also, because the various theoretical models make predictions as to how the rate of proton transfer should vary with a change in free energy for reaction as well as how the rate constant should vary with solvent, it is desirable to study molecular systems where both the free energy change for reaction and the solvent can be varied.

In an initial report, we presented the findings of a picosecond kinetic study of the dynamics of proton transfer within contact radical ion pairs formed between the radical cation of dimethylaniline and the radical anion for a variety of substituted benzophenones.[30] We examined how the reaction dynamics varied with change in free energy for reaction as well with solvent, and found that the kinetic behavior is in qualitative accord with the predictions of Borgis−Hynes theory for nonadiabatic proton transfer.[7] In this report, we extend our initial studies to further examine Borgis−Hynes theory by probing the reaction dynamics of proton transfer within substituted benzophenones/diethylaniline contact radical ion pairs in the solvents benzene and cyclohexane.

## Experimental Section

The substituted benzophenones (4,4′-methoxy, 4-methoxy, 4-methyl, 4-fluoro, 4-chloro, and 4,4′ -dichloro) were obtained from Aldrich, and 4,4′-dimethylbenzophenone was obtained from Kodak. Each of the substituted benzophenones was recrystallized from ethanol and dried under vacuum. *N*,*N*-Diethylaniline, also obtained from Aldrich, was distilled from calcium hydride under vacuum and stored under argon to prevent the development of oxidation products. The solvents cyclohexane (Mallinckrodt) and benzene (Baker) were used as received.

The picosecond absorption spectrometer is based on a Continuum (PY61C-10) Nd:YAG laser that produces 19-ps light pulses at 1060 nm. The second harmonic, 530 nm, was focused into an $H_2O/D_2O$ cell, which was used to generate a white light continuum. A 5-nm band-pass filter was used to select the 680 nm probe light. The third harmonic, 355 nm, was used to initiate the chemistry. The I and $I_o$ probe beams were detected by two photodiodes, Oriel 71902 UV-enhanced, which are interfaced to a Stanford (SRS 250) boxcar integrator, and the data were transferred to a computer. The samples, whose temperature were held at 23 °C, flowed through a cuvette to prevent the build up of photoproducts. The method of deconvolution of the kinetic data has been presented.[31]

## Results and Discussion

**Dynamics of Proton Transfer.** To assess the validity of recently developed theoretical models for proton transfer in the condense phase, the experimental system must meet several criteria. First and foremost, the kinetic process under observation must be solely ascribed to proton transfer. For photochemically induced processes, this criterion has been problematic, because electron-transfer reactions as well as radiative and nonradiative decay processes are competing with proton-transfer processes. Furthermore, if the rate of proton transfer is to be examined as a function of the change in free energy, the most convenient method for effecting this change is by the utilization of substituent effects. However, when substituents are employed

10.1021/jp9939672 CCC: $19.00 
Published on Web 04/29/2000

**SCHEME 1**

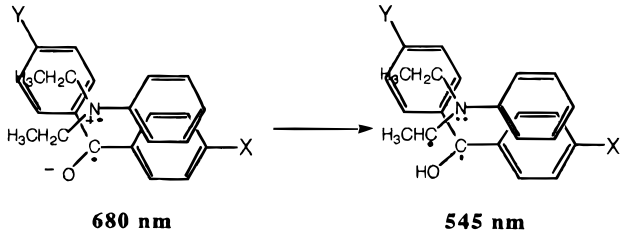


to vary the free energy change, it is important that the distance of proton-transfer remain constant with the change in substituents. Finally, the experimental system must be soluble in a wide range of solvents.

Proton transfer within the contact radical ion pair composed of the radical cation of diethylaniline and the radical anion of substituted benzophenones meet these established criteria. When benzophenone and it various derivatives are irradiated at 355 nm, the triplet state is produced within 10 ps.[31] In the presence of the appropriate concentration of the aromatic amine in a nonpolar solvent, an electron is then transferred to the triplet state of the ketone to produce the contact radical ion pair, whose spin state is also a triplet; employing nonpolar solvents is critical so as to avoid the production of solvent-separated radical ion pairs.[32,33] The amine concentration is also important for the sole production of the triplet contact radical ion pair; at too high a concentration, electron-transfer becomes competitive with intersystem crossing of the ketone, thus giving rise to singlet radical ion pairs that may undergo rapid back electron transfer to produce ground-state reactants.[33] On the picosecond time scale, the only reaction to occur within the triplet contact radical ion pair in a nonpolar solvent is the transfer of a proton from the radical cation of the aromatic amine to the radical anion of the ketone to produce the ketyl radical. Back electron transfer and ion pair diffusional separation are not competitive because these processes occur on a long time scale (>10 ns).[31]

The geometry of the triplet contact radical ion pair for benzophenone/diethylaniline has not been determined and thus can only be surmised. From numerous studies of excimers and exciplexes, the most stable structure to maximize the Coulombic attraction would be that of a $\pi$-stack (Scheme 1).[34]

From studies of excimers and exciplexes, the estimated distance between the two moieties should be of the order 3.3 Å.[34] Assuming this structure for the contact radical ion pair, when substituents are added to the 4,4′ positions (X,Y in Scheme 1) of benzophenone so as to vary the energetics for proton transfer, the separation of the $\pi$-stack should be minimally perturbed because the substituents are in line with the plane of the aromatic rings of benzophenone and should not come into van der Waal's contact with the aromatic amine.

For the following series of experiments, the concentrations employed were 0.02 M for the benzophenones and 0.4 M for diethylaniline in the solvents benzene and cyclohexane. The kinetics for proton transfer, which were derived from the decay of the radical anion of the benzophenones monitored at 680 nm (Scheme 1), were found to be independent of the concentration of the amine over the range 0.2−0.4 M. At higher concentrations of amine, the decay of the radical anion becomes concentration dependent, reflecting the production of singlet radical ion pairs and their ensuing dynamics. The acquisition of the kinetic data utilized 80 time points in 25-ps time increments, allowing the reactions to be monitored up to 2 ns. The modeling of the kinetic data assumed a single-exponential decay for the evolution of the triplet contact radical ion pair into the radical pair through proton transfer (Scheme 1). An example of the fit of this kinetic model to the experimental data for 4,4′-dimethoxybenzophenone/diethylaniline is shown in Figure 1. The results for each of the systems are given in Table 1.

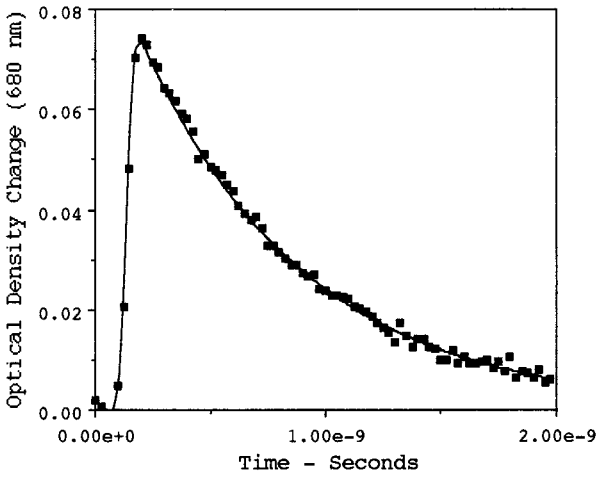


**Figure 1.** Transient absorption at 680 nm following 355 nm excitation of 0.02 M 4,4′-dimethoxybenzophenone−0.4 M *N*,*N*-diethylaniline in benzene. $k_{pt} = 1.4 \times 10^9$ s$^{-1}$; pulse width, 25 ps; $t_o = 1.5 \times 10^{-10}$ s) Key: (squares) experimental points; (solid line) fit to data.

**TABLE 1: Observed Rate Constants for the Decay of Substituted Benzophenones/Diethylaniline Triplet Radical Ion Pair (at 23 °C)**

| 4,4′-benzophenone | | cyclohexane | benzene |
|---|---|---|---|
| 4 | 4′ | $k_H$ ($10^9$ s$^{-1}$)[a] | $k_H$ ($10^9$ s$^{-1}$) |
| $CH_3O$ | $CH_3O$ | 1.2 | 1.4 |
| $CH_3$ | $CH_3$ | 2.3 | 2.0 |
| $CH_3O$ | H | 2.3 | 1.9 |
| $CH_3$ | H | 3.5 | 1.9 |
| H | H | 4.5 | 1.6 |
| F | H | 4.6 | 1.4 |
| Cl | H | 3.3 | 1.3 |
| Cl | Cl | 2.5 | 1.3 |

[a] Estimated uncertainties in rate constants ±10 (1$\sigma$).

We also attempted to study the proton-transfer process in the polar solvents dichloroethylene and dimethylformamide. However, following the production of the radical anion of benzophenone in these solvents, there was a varying time delay of 50 to 100 ps before the radical anion began to decay by proton transfer. This delay time could reflect the initial production of solvent-separated radical ion pairs, which must then be transformed into the contact radical ion pair prior to proton transfer. Given the additional kinetic complexity manifested in these polar solvents, we decided to limit this investigation to the nonpolar solvents benzene and cyclohexane.

**Borgis−Hynes Theory.** A common feature in all of the kinetic theories developed in the past 20 years for proton transfer recognize the importance of solvent fluctuations in promoting the reaction process.[4,7,9,10] Given that the charge distribution in the reactant will vary relative to that for the product, then the solvent structure around the reactant will differ from that around the product. Therefore, as in electron transfer, a critical component to the overall reaction coordinate is a fluctuation in the solvent structure during reaction, a process that will normally be thermally activated.

Another important component governing the dynamics of proton transfer is the nature of the electronic coupling between the reactant and the product states.[4,7] At large distances, the electronic coupling will be weak, resulting in an electronic

barrier in the proton transfer reaction coordinate. In the weak coupling limit or the nonadiabatic limit, the proton transfers from the reactant state to the product state through a tunneling process. However, as the distance for proton transfer decreases, the coupling between the reactant state and product state increases, leading to a reduction in the electronic barrier in the proton transfer coordinate. When the distance is sufficiently small, the electronic barrier between the reactant and product states falls below the zero point energy of the proton vibration, thus achieving the adiabatic limit; that is, there is no electronic barrier in the proton transfer coordinate. The distance that marks the separation between the nonadiabatic and adiabatic limits cannot be easily characterized and will be system specific. However, from model calculations, distances on the order of 2.5 Å serve to separate the adiabatic and nonadiabatic regimes.[7]

Finally, Borgis and Hynes have addressed the issue of the importance of low-frequency vibrational modes in promoting proton transfer in the nonadiabatic limit.[7] The magnitude of the tunneling matrix element has the analytical form of $C(Q) = C_o\exp(-\alpha\ \delta Q)$, where $C_o$ is the value of the tunneling matrix element at the equilibrium position of the vibrational promoting mode, $Q_o$, and $\delta Q$ is a measure of the displacement of the promoting mode. The term $\alpha$ is a parameter that specifies the sensitivity of the tunneling term to the displacement $\delta$Q. For proton transfer, this parameter may vary from 25 to 35 Å$^{-1}$, which is very much larger than the corresponding parameter found in electron transfer theory where the $\alpha$ term for the fall off of the electronic coupling is $\sim$1 Å$^{-1}$.[7] It is this extreme sensitivity of the tunneling matrix element to $\delta Q$ that mandates the incorporation of a low-frequency promoting mode into the kinetic theory for nonadiabatic proton transfer.

The Borgis−Hynes model introduces a low-frequency vibrational mode $Q$, whose frequency is $\omega_Q$, and the associated vibrational reorganization energy is $E_v$.[7] Based on a Landau−Zener curve crossing model, they derived the nonadiabatic rate constant, $k$;

$$k = (2\pi\beta/h)(\pi/\beta E_s)^{1/2} \sum_n \sum_m P_n C_{nm}{}^2 \exp(-\beta\Delta G_{nm}{}^{\ddagger}) \quad (1)$$

The activation free energy is given by

$$\Delta G_{nm}{}^{\ddagger} = (1/4E_s)(E_s + \Delta E + \Delta E_{nm})^2 \quad (2)$$

where $E_s$ is the solvent reorganization energy, $\Delta E$ is the energetics of the reaction asymmetry, and $\Delta E_{nm}$ is the vibrational asymmetry on going from the $n$ vibrational level in the reactant state to the $m$ vibrational level in the product state. The parameter $P_n$ is the Boltzman expression for the thermal average over the thermal populations for the $n$ vibrational level in the reactant state. The tunneling term, $C_{nm}$, is the coupling matrix element between the $n$-vibrational level in the reactant state with the $m$-vibrational level in the product state, which is dependent on a promoting vibration $Q$,

$$C_{nm}{}^2 = C_0{}^2 \exp(-\alpha\Delta Q_e) \exp((E_\alpha - E_v)/h\omega_Q) F[L(E_v, E_\alpha, \omega_Q)] \quad (3)$$

The energy $E_\alpha$ is a quantum term associated with the proton reaction coordinate coupling to $Q$ vibration, $E_\alpha = h^2\alpha^2/2m$; $\Delta Q_e$ is the shift in the $Q$ oscillator equilibrium position upon reaction; $C_0$ is the tunneling matrix element for the transfer from the 0 vibrational level in the reactant state to the 0 vibrational level in the product state; and $F[L(E_Q, E_\alpha, \omega_Q)]$ is a function of a Laguerre polynomial (see ref 7).

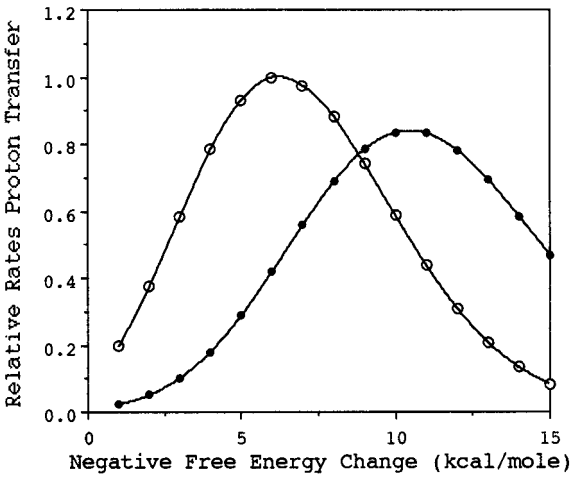


**Figure 2.** Graph of free energy dependence ($-\Delta G$ kcal/mol) of the relative rates of proton transfer employing the Borgis−Hynes model (eqs 1−3), where $E_\alpha$ = 2.0 kcal/mol, $E_Q$ = 1.0 kcal/mol, and the vibrational frequency is 600 cm$^{-1}$. Key: (open circles) $E_s$ = 1.0 kcal/mol; (filled circles) $E_s$ = 5.0 kcal/mol.

A telling feature that distinguishes the theory for nonadiabatic proton transfer, in its many theoretical formulations, from Transition State Theory is the relationship between the rate of proton transfer and the free energy change for the reaction. Nonadiabatic theories have the unique prediction that initially, as the free energy for reaction becomes more negative, the rate constant for the reaction increases but, at some point, this relationship changes to where a further increase in negative free energy change for reaction leads to a decrease in the rate constant for reaction, reminiscent of the functional form for nonadiabatic electron-transfer processes. Employing Borgis−Hynes theory for nonadiabatic proton transfer, the dependence of rate constant on free energy change as function of the solvent reorganization energy is presented in Figure 2.[7] In this series of calculations, the rate constants are normalized by $k/\{C_o{}^2 \exp(-\alpha\Delta Q_e)\}$ and then again further normalized by having the largest rate constant set equal to 1.0. In both sets of calculations, the vibrational reorganization energy, $E_v$, is 1.0 kcal/mol, the quantum term $E_\alpha$ is 2.0 kcal/mol, and the promoting mode $\omega_Q$ corresponds to 600 cm$^{-1}$; the only difference in the two calculations is the curve with the largest rate constant has a solvent reorganization energy, $E_s$, of 1.0 kcal/mol, wherease the second curve has an $E_s$ of 5.0 kcal/mol. Increasing the solvent reorganization energy by 4 kcal/mol leads to an approximate shift between the two curves of 4 kcal/mol. The position in the maximum rate for proton transfer is a sensitive function of the values for the parameters $E_s$, $E_v$, $E_\alpha$, and $\omega_Q$. The width in the distribution of rate constants is only weakly sensitive to these parameters. Finally, there is a reduction in the maximum rate constant with an increase in $E_s$, which can be attributed in part to the term of $E_s{}^{1/2}$ in eq 1. Therefore, the experimental signature for nonadiabatic proton transfer is the existence of an "inverted region".

**Determination of the Energetics for Proton Transfer.** To assess the applicability of either Transition State Theory or nonadiabatic proton transfer theory to the observed reaction dynamics within the benzophenone/diethylaniline contact radical ion pair, the correlation of the rate constant for proton transfer with the change in free energy needs to be examined. Unfortunately, a direct measurement of the energetics associated with the proton transfer within the contact ion pair occurring on the picosecond time scale is problematic; therefore it is necessary to estimate the associated energetics.

The first step in determining how the energetics for proton transfer changes with both substituents and solvent involves establishing the energetics of the contact radical ion pair and the radical pair relative to the ground-state reactants; their resulting difference reflects the change in free energy for the reaction. Mataga and co-workers determined that the energy of the contact radical ion pair for benzophenone/diethylaniline in acetonitrile is 58.4 kcal/mol.[32] The solvent dependence of the contact radical ion pair can then be estimated based on the work of Gould, Goodman, Farid and co-workers, who established how the energy of the contact radical ion pair of 1,2,4,5-tetracyanobenzene/hexamethylbenzene varies in a variety of solvents.[35] From a correlation of solvent $E_T$ 30 values with the change in solvation energy, one can estimate how much the contact radical ion pair is destabilized, relative to acetonitrile, in the solvents benzene and cyclohexane. We find that, relative to acetonitrile, the energy of the contact radical ion pair increases by 2.8 kcal/mol in benzene and by 3.6 kcal/mol in cyclohexane.

The energy for the radical pair relative to benzophenone/diethylaniline is determined from literature values for the energy for the formation of the benzophenone ketyl radical[36] and the C—H bond dissociation energy of diethylaniline.[37] Employing the following thermodynamic cycle

$$(C_6H_5)_2C{=}O + H_2 \rightarrow (C_6H_5)_2CHOH \quad \Delta H = -9 \text{ kcal/mol}$$
$$2H\cdot \rightarrow H_2 \quad \Delta H = -104 \text{ kcal/mol}$$
$$(C_6H_5)CHOH \rightarrow H\cdot + (C_6H_5)_2COH \quad \Delta H = 78 \text{ kcal/mol}$$
$$\text{diethylaniline} \rightarrow + H\cdot(C_6H_5)N(CH_3CH_2)(CH_3CH_2\cdot) \quad \Delta H = 91.7 \text{ kcal/mol}$$

$$\text{benzophenone} + \text{diethylaniline} \rightarrow (C_6H_5)_2COH + (C_6H_5)N(CH_3CH_2)(CH_2CH\cdot) \quad \Delta H = 56.7 \text{ kcal/mol}$$

we find that the energy change associated with the transfer of a proton in the benzophenone/diethylaniline contact radical ion pair is exothermic by 1.7 kcal/mol (58.4 kcal/mol − 56.7 kcal/mol) in acetonitrile. In benzene, this value increases to 4.5 kcal/mol, and in cyclohexane, the value is 5.3 kcal/mol. This calculation assumes that the energy of the radical pair is insensitive to solvent.

The effect of substituents on the energy of the benzophenone/diethylaniline contact radical ion pair is estimated from the measurement of the reduction potentials of substituted benzophenones. Arnold and co-workers measured the reduction potential for a number of 4,4′-substituted benzophenones and found an excellent correlation between the reduction potential and Hammett $\sigma$ parameter.[38] Based on reduction potentials, the 4-fluoro, 4-chloro, and 4,4′-dichloro substituents stabilize the contact radical ion pair by 0.5, 1.9, and 4.0 kcal/mol, respectively. The remaining substituents destabilize the contact radial ion pair by 0.9 kcal/mol for 4-methyl, 2.1 kcal/mol for 4-methoxy, 2.1 kcal/mol for 4,4′-dimethyl, and 4.4 kcal/mol for 4,4′-dimethoxy.

Estimating the effect of substituents on the energy of the radical ion pair is much more difficult and a direct measure has not been achieved. However, the effect of substituents on the stability of a carbon center radical can be estimated from the kinetic data obtained by Creary for substituent effects on kinetics for the thermal isomerization of 2-aryl-3,3-dimethylmethylenecyclopropanes, where it is assumed that the mechanism involves a biradical intermediate.[39] The kinetic data can be transformed into an enthalpy of activation, which reflects the effect of substituents on radical stability by assuming an $A$ factor of $10^{14}$ $s^{-1}$ for the thermal rearrangement.[40] Because the benzophenone ketyl radical is a more highly delocalized radical compared with the radical generated in the isomerization just mentioned, we arbitrarily assume that the substituent effect on ketyl radical stability will be reduced by 50%. Thus, the derived substituents effects on the stability of the ketyl radical, which are stabilizing, are as follows: 4,4′-dimethoxy (0.4 kcal/mol), 4,4′-dimethyl (0.2 kcal/mol), 4-methoxy (0.2 kcal/mol), 4-methyl (0.1 kcal/mol), 4-chloro (0.1 kcal/mol) and 4,4′-dichloro (0.2 kcal/mol). The only substituent that destabilizes the ketyl radical is the 4-fluoro (−0.1 kcal/mol).

**TABLE 2: Effect of Substituents on the Energetics for Proton Transfer**

| 4,4′-benzophenone | | | |
|---|---|---|---|
| 4 | 4′ | $C_6H_6$ (kcal/mol)[a] | $C_6H_{12}$ (kcal/mol)[b] |
| $CH_3O$ | $CH_3O$ | −9.3 | −10.1 |
| $CH_3$ | $CH_3$ | −6.8 | −7.6 |
| $CH_3O$ | H | −6.8 | −7.6 |
| $CH_3$ | H | −5.5 | −6.3 |
| H | H | −4.5 | −5.3 |
| F | H | −3.9 | −4.7 |
| Cl | H | −2.7 | −3.5 |
| Cl | Cl | −0.7 | −1.5 |

[a] Benzene. [b] Cyclohexane.

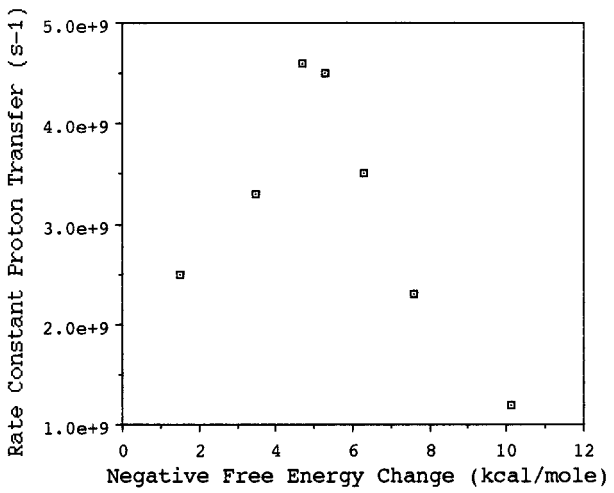


**Figure 3.** Plot of the rate constant for proton transfer versus free energy change ($-\Delta G$ kcal/mol) for the solvent cyclohexane.

Combining the data for solvent effects on contact ion pair stabilities, substituent effects on contact ion pair, and substituent effects on radical pair stabilities leads to a determination of the energetics for proton transfer within the contact radical ion pair, Table 2.

**Comparison of Theory and Experiment.** The correlation of the rate constants for proton transfer with the change in energy for the solvents cyclohexane and benzene can be found in Figures 3 and 4. In cyclohexane, the rate constant increases as the energy for reaction increases from −1.5 to −4.7 kcal/mol, and then decreases as the energy for reaction further increases to −10.1 kcal/mol. Similarly, in benzene, the rate constant for proton transfer increases as the reaction energy increases from −0.7 to −6.9 kcal/mol, and then in turn decreases as the reaction energy further increases to −9.3 kcal/mol. Clearly, in both solvents, there is evidence for an inverted region for proton transfer, suggesting that reaction process indeed involves nonadiabatic proton transfer.[7] Transition State Theory cannot account for this behavior.

A question that does arise is whether this process is nonadiabatic, (i.e., the proton is tunneling) or whether the

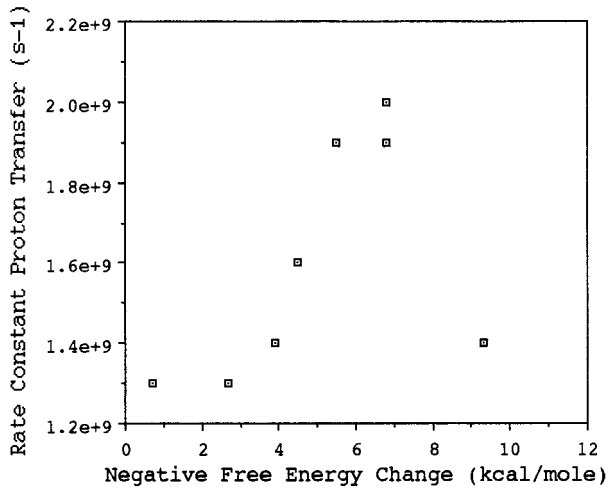


**Figure 4.** Plot of the rate constant for proton transfer versus free energy change ($-\Delta G$ kcal/mol) for the solvent benzene.

process may be adiabatic in the proton coordinate, (i.e., there is no electronic barrier in the proton reaction coordinate). Borgis and Hynes[7] have developed a theoretical formalism for adiabatic proton transfer that results in with the following equation:

$$k_{ad} = (\omega_s/2\pi) \exp(-\beta \Delta G^{\ddagger}) \quad (4)$$

where $\omega_s$ is the solvent frequency and $\Delta G^{\ddagger}$ is the free energy of activation. The maximum in the rate for proton transfer, which occurs when $\Delta G^{\ddagger} = 0$ kcal/mol, will then be of the order $\omega_s/2\pi$, which for most nonhydrogen-bonding solvents should be $>10^{12}s^{-1}$. However, the maximum rate for proton transfer in cyclohexane is $4.6 \times 10^9$ s$^{-1}$ and in benzene is $2.0 \times 10^9$ s$^{-1}$. These rates are >2 orders of magnitude slower than that expected for an adiabatic process, thus further support a nonadiabatic model for the proton-transfer process.

Two interesting features that are manifested in the experimental data depicted in Figures 3 and 4 are the relative positions of the two maxima in both the rate and energy coordinates. In the energy coordinate, the benzene maximum is shifted to higher energies relative to the cyclohexane maximum by ~2.0 kcal/mol, whereas the maximum rate constant in benzene is reduced by a factor of 2.3 relative to cyclohexane. If one assumes that only $E_s$ changes when the solvent changes from cyclohexane to benzene, then the difference in the two maxima reflect the difference in the solvent reorganizations of cyclohexane and benzene (see Figure 2). Unfortunately, we can think of no method that would allow an independent determination of $E_s$ for proton transfer in these solvents. The decrease, by a factor of 2.3, in the maximum rate for proton transfer when the solvent cyclohexane is replaced by benzene is rationalized with the aid of eq 1, which contains the prefactor term $E_s^{-1/2}$. As solvent reorganization energy increases, which should occur when cyclohexane is replaced by benzene, the maximum rate constant should decrease. Another possible contribution to the decrease in the rate constant may result from a change in the tunneling matrix element with solvent. Given the greater polarity of benzene relative to cyclohexane, the intermolecular distance within the contact radical ion pair should be greater in benzene, leading to a decrease in the magnitude of the tunneling matrix element.

A comparison of our previous study of proton transfer within the benzophenone/dimethylaniline contact radical ion pairs[30] with the present results can be viewed in Figures 5 and 6. In the solvent cyclohexane (Figure 5), the maximum rate constant

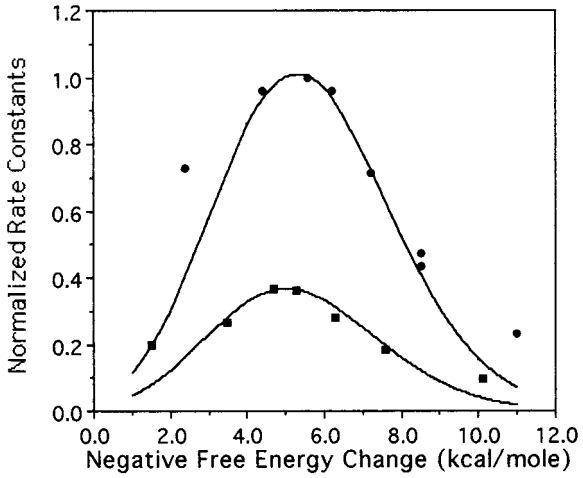


**Figure 5.** Plot of the normalized rate constants for proton transfer versus free energy change (-$\Delta G$ kcal/mol) for the solvent cyclohexane. All of the experimental rate constants have been normalized to the maximum rate constant found for 4-fluoro-benzophenone/dimethylaniline ($12.5 \times 10^9$ s$^{-1}$) in cyclohexane (see ref 30). The theoretical rate constants have been normalized to the respective experimental data. Key: (circles) experimental data for substituted benzophenones/dimethylaniline;[30] (squares) experimental data for substituted benzophenones/diethylaniline. Solid curves are calculated rate constants for proton transfer based on eq 1. Curve through circles: $E_s = 1.25$ kcal/mol, $E_v = 1.0$ kcal/mol, $E_\alpha = 1.0$ kcal/mol, $\omega_Q = 300$ cm$^{-1}$, and $T = 298$ K. Curve through squares: $E_s = 1.0$ kcal/mol, $E_v = 1.0$ kcal/mol, $E_\alpha = 1.0$ kcal/mol, $\omega_Q = 300$ cm$^{-1}$; and $T = 298$ K.

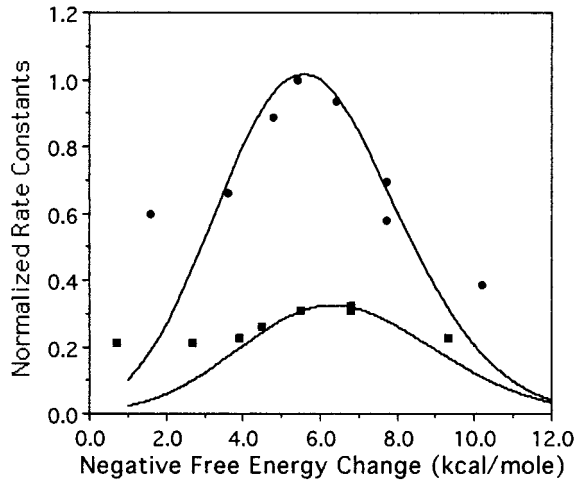


**Figure 6.** Plot of the normalized rate constants for proton transfer versus free energy change (-$\Delta G$ kcal/mol) for the solvent benzene. All of the experimental rate constants have been normalized to the maximum rate constant found for benzophenone/dimethylaniline ($6.2 \times 10^9$ s$^{-1}$) in benzene (see ref 30). The theoretical rate constants have been normalized to the respective experimental data. Key: (circles) experimental data for substituted benzophenones/dimethylaniline;[30] (squares) experimental data for substituted benzophenones/diethylaniline. Solid curves are calculated rate constants for proton-transfer based on eq 1. Curve through circles: $E_s = 1.5$ kcal/mol, $E_v = 1.0$ kcal/mol, $E_\alpha = 1.0$ kcal/mol, $\omega_Q = 300$ cm$^{-1}$, and $T = 298$ K. Curve through squares: $E_s = 2.0$ kcal/mol, $E_v = 1.0$ kcal/mol, $E_\alpha = 1.0$ kcal/mol, $\omega_Q = 300$ cm$^{-1}$, and $T = 298$ K.

for proton transfer within the benzophenone/diethylaniline contact radical ion pairs is a factor of 0.37 smaller than that found for the benzophenone/dimethylaniline contact radical ion pairs. Similarly, in benzene (Figure 6), the maximum rate is again reduced by a factor of 0.32 for the same comparison. In cyclohexane, the shapes of the two curves are remarkably similar, whereas in benzene there is a greater difference in the

shape for the two sets of experimental data. These differences may reflect errors in the determination in the rate constants for proton transfer as well the energetics for proton transfer. Most interesting, however, is the reduction in the maximum rate constant when the amine is changed from dimethylaniline to diethylaniline. Because the rate constant for proton transfer is exquisitely sensitive to distance in the tunneling regime, the smaller rate constants for proton transfer within the benzophenone/diethylaniline contact radical ion pair may reflect a slightly larger average internuclear separation of the contact radical ion pair, which may be attributed to the additional two methyl substituents, comparing diethyl with dimethyl.

Finally, the question arises as to whether the Borgis−Hynes theoretical formulation can quantitatively account for the observed kinetic behavior of the two molecular systems that have been studied. A comparison of Borgis−Hynes theory with experiment is give in Figures 5 and 6. The parameters utilized in obtaining the theoretical curves are given in the figure captions. These fitting parameters are not unique in the sense that the maximum in the theoretical curve is a function of all of the parameters, which are interdependent. The theoretical curves have been normalized to the maximum rate constant for the experimental data because an absolute determination of the rate constant given by eq 1 is not feasible given our inability to calculate the tunneling matrix element, $C_o$, as well as estimate the magnitude of the shift of the $Q$ oscillator, $\Delta Q_e$. For the solvent cyclohexane, the fit of the theoretical model to both sets of experimental data is rather good over the range of −4 to −9 kcal/mol; slight deviations are observed between theory and experiment over the ranges of −1 to −4 kcal/mol and −9 to −11 kcal/mol, where theory underestimates the experimental rate data by a factor of at least 2. For benzene, there is again good agreement between theory and experiment over the range of −4 to −8 kcal/mol. However, from −1 to −4 kcal/mol and from −8 to −11 kcal/mol, there is significant deviation in the fit; theory underestimates the experimental rate data by a factor of at least 3. The deviation between Borgis−Hynes theoretical model and the present experimental data is perhaps not surprising given that the theoretical formulation given by eq 1 is based on a model in which there is only one promoting vibration $Q$. However, for the contact radical ion pairs employed in these two studies, several low-frequency vibrational modes will serve to reduce the distance between the two heavy atoms between which the proton tunnels. Therefore, the deviation between the theoretical model and experiment may be the result of several of the vibrational modes being active in promoting proton transfer. Thus, a more complete theoretical model should allow for a summation over many promoting vibrational modes as well as excitation in the proton bending and stretching vibrational modes. However, it is still remarkable that a theory based on just one promoting model is in qualitative accord with the experimental data.

In conclusion, although it is not possible to rigorously assess the validity of Borgis−Hynes theory for nonadiabatic proton transfer employing the present experimental system, given the great number of parameters necessary to calculate the rate of proton transfer as well as the possible intervention of several vibrational modes promoting proton transfer, the dynamic behavior of the present experimental system seems to be in qualitative accord with theoretical predictions. Most importantly, the shape of the rate-free energy curves, the shift in the maximum to higher energy with increasing solvent reorganization energy, and a decrease in rate constant for proton transfer with increasing solvent reorganization energy support a nonadiabatic theoretical model.

**Acknowledgment.** This work is supported by grants from the National Science Foundation, CHE −9816540, and University of Colorado Council on Research and Creative Work.

## References and Notes

(1) Babamow, V. K.; Marcus, R. A. *J. Chem. Phys.* **1981**, *74*, 1790.
(2) Garrett, B. C.; Truhlar, D. G.; Wagner, A. F.; Dunning, T. *J. Chem. Phys.* **1983,** *78*, 4400.
(3) Truhlar, D. G.; Garrett, B. C. *Acc. Chem. Res.* **1980**, *14*, 440.
(4) Kuznetsov, A. M. *Charge Transfer in Physics, Chemistry and Biology;* Gordon and Breach: Luxembourg, 1995.
(5) Borgis, D. C.; Lee, S.; Hynes, J. T. *Chem. Phys. Letts*. **1989**, *162*, 19.
(6) Borgis, D.; Hynes, J. T. *J. Chem. Phys.* **1991**, *94*, 3619.
(7) Borgis, D.; Hynes, J. T. *J. Phys Chem*. **1996,** *100*, 1118.
(8) Cukier, R. I.; Morillo, M. *J. Chem. Phys.* **1989**, *91*, 857.
(9) Morillo, M.; Cukier, R. I. *J. Chem. Phys.* **1990**, *92*, 4833.
(10) Li, D.; Voth, G. A. *J. Phys. Chem.* **1991,** *95*, 10425.
(11) Lobaugh, J.; Voth, G. A. *J. Chem. Phys.* **1994,** *100*, 3039.
(12) Gandour, R. D.; Schowen, R. L. *Transition States of Biochemical Processes*; Plenum: New York, 1978.
(13) Bell, R. P. *The Tunnel Effect in Chemistry*; Chapman and Hall: London, 1980.
(14) Westheimer, F. H. *Chem. Rev.* **1961**, *61*, 265.
(15) Bell, R. P. *The Proton in Chemistry*; Chapman and Hall: London, 1973.
(16) Fresht, A. *Enzyme Structure and Mechanism*; W. H. Freeman: New York, 1985.
(17) Barbara, P. F.; Walsh, P. K.; Brus, L. E. *J. Phys. Chem.* **1989**, *93*, 29
(18) Lawrence, M.; Marzzacco, C.; Morton, C.; Schwab, C.; Halpern, A. M. *J. Phys. Chem*. **1991**, *95*, 10294.
(19) Tolbert, L. M.; Nesselroth, S. M. *J. Phys. Chem.* **1991**, *95*, 10331.
(20) Moog, R. S.; Maroncelli, M. *J. Phys. Chem.* **1991,** *95*, 10359.
(21) Robinson, G. W. *J. Phys. Chem.* **1991**, *95*, 10386.
(22) Shida, N.; Almlof, J.; Barbara, P. F. *J. Phys. Chem.* **1991**, *95*, 10457.
(23) Pines, E.; Fleming, G. R. *J. Phys. Chem.* **1991**, *95*, 10448.
(24) Zewail, A. H. *J. Phys. Chem*. **1996,** *100*, 12701.
(25) Hineman, M. F.; Bruker, G. A.; Kelley, D. F.; Bernstein, E. R. *J. Chem. Phys.* **1990,** *92*, 805.
(26) Syage, J. A. *J. Phys. Chem.* **1995,** *99*, 5772.
(27) Brucker, G. A.; Swinney, T. C.; Kelley, D. F. *J. Phys. Chem*. **1991,** *95*, 3190.
(28) Swinney, T. C.; Kelley, D. F. *J. Chem. Phys*. **1993**, *99*, 211.
(29) Dreyer, J.; Peters, K. S. *J. Phys. Chem.* **1996,** *100*, 19412.
(30) Peters, K. S.; Cashin, A.; Timbers, P. *J. Am. Chem. Soc*. **2000**, *122*, 107.
(31) Peters, K. S.; Lee, J. *J. Phys. Chem*. **1993**, *97*, 3761.
(32) Miyasaka, H.; Kiri, M.; Morita, K.; Mataga, N.; Tanimoto, Y. *Chem. Phys. Lett.* **1992**, *199*, 21.
(33) Miyasaka, H.; Nagata, T.; Kiri, M.; Mataga, N.*J. Phys. Chem.* **1992,** *96*, 8060.
(34) Birks, J. B. *The Photophysics of Aromatic Excimers*; Birks, J. B., Ed.; Academic: New York, 1975.
(35) Gould, I. R.; Noukakis, D.; Gomez-Jahn, L.; Young, R. H.; Goodman, J. L.; Farid, S. *Chem. Phys.* **1993,** *176*, 439.
(36) Walling, C.; Gibian, M. J. *J. Am. Chem. Soc*. **1965**, *87*, 3361.
(37) Dombrowski, G. W.; Dinnocenzo, J. P.; Farid, S.; Goodman, J. L.; Gould, I. R. *J. Org. Chem.* **1999,** *64*, 427.
(38) Leigh, W. J.; Arnold, D. R.; Humphreys, R. W. R.; Wong, P. C. *Can. J. Chem*. **1980**, *58*, 2537.
(39) Creary, X. *J. Org. Chem.* **1980,** *45*, 280.
(40) Kirmse, W. J. C. S. *Chem. Commun.* **1977**, 122.